Ionization via high-Rydberg states with multiple V-type resonances

R. Parzyński and A. Grudka
Quantum Electronics Laboratory, Institute of Physics, A. Mickiewicz University, Umultowska 85, 61-614 Poznań, Poland
(Received 12 February 1998)

We study an extended model of intense-laser ionization of the hydrogenlike atom from a low excited state via a band of high Rydberg states. The essence of the extension is that the population from the directly excited low-angular-momentum Rydberg band is allowed to migrate resonantly toward Rydberg bands of higher angular momenta through a sequence of V-type degenerate Raman transitions. Each V-type transition exploits, as a resonant intermediary, the state of the same principal quantum number as that of the initial state but of a different angular momentum number. We find an analytical limit to this model, and obtain for it a closed-form solution for arbitrary length of the chain of the V-type transitions. This solution implies that, through the chain of V-type resonances, the population initially localized in a single state can be spread over a number of bound states of much higher angular momenta. The main result of the model is that, at high intensities, no population is left in high Rydberg states, but the population not released to the continuum is shared between the initial state and the higher-angular-momentum states of the same energy as that of the initial state. This sharing depends on the pulse duration, and, for the duration approaching one Kepler period of the resonantly excited high Rydberg state, the initial state was found to be completely depleted. This particular result emphasizes the effect of the orbital degeneracy of the initial level and V-type resonances on the high-intensity hydrogen-atom stabilization. [S1050-2947(98)00608-8]

PACS number(s): 42.50.Hz, 32.80.Rm

I. INTRODUCTION

The paper is an extension of the discussion we presented in Sec. II C of our previous paper [1], in which we introduced a model of nominal two-photon ionization by a strong light pulse of the hydrogenlike atom from an isolated initial state via a band of high Rydberg states. The interesting element was the inclusion of resonant migration of the population from the directly excited Rydberg band of a given angular-momentum quantum number toward the Rydberg band of an angular momentum quantum number higher by 2. The channel of migration was a V-type degenerate Raman transition between the two Rydberg bands via a state of the principal quantum number the same as that of the initial state but of a different angular momentum quantum number.

Previously [1] we allowed only one V-type resonance, and now we wish to generalize this simplest model to include a sequence of V-type resonances linked in a chain. Due to its orbital degeneracy, the hydrogen atom allows a number of such coupled resonances, particularly when the initial state is of a relatively high principal quantum number and, at the same time, of a low angular momentum quantum number. The main questions we raise in the framework of the generalized model concern (a) the efficiency of the migration of the population toward the bound states of angular momenta much higher than that of the initial state, (b) the ability of the initial state to survive the laser pulse, (c) the possibility for bound states different from the initial one to trap population, and (d) the effect of stabilization against ionization. We find answers to these questions considering a fully analytically solvable limiting case of the model, i.e., when bound-bound and bound-free matrix elements of the atom-field couplings are roughly assumed to be independent of the angular momentum quantum number l. The results obtained suggest that the migration of population toward higher-l bound states (both low and high) via a sequence of V-type resonances can be non-negligible provided that the pulse duration is not too short when compared to the classical Kepler period of the high Rydberg states directly excited from the low initial state. If the pulse is short, the model predicts that the initial state has the property of surviving it even if it is of high intensity. A substantial difference is found in the behavior of the population between high Rydberg states and low states of the same energy as the initial one but of higher angular momenta. At high intensities, the former are practically completely depopulated, but the latter trap some population. As a result, the high-intensity stabilization occurring against ionization is seen as an interplay between the initial-state survival and trapping some population in higher-l states of the same energy as that of the initial state. All this suggests that simpler models not including the coupled V-type resonances, if allowed by the selection rules, may not always give reliable results. We find, however, that predictions of our extended model are highly sensitive to the atom-field coupling parameters.

The paper is organized as follows. Section II presents a generalized model and the scheme of its solution, forming the basis for future numerical analysis. In Sec. III, we focus on a particular version of our model, for which we find a fully analytical solution for an arbitrary number of V-type transitions in the coupling chain. As an illustration of our analytical solution, in Sec. IV we discuss results for the model with three V-type resonances. We end the paper with a short summary in Sec. V.

II. MODEL AND SOLUTION SCHEME

Let the hydrogen atom be initially in the state $|\lambda=1\rangle = |n_1, l_1>0, m_1=l_1-1\rangle$ (the black dot in Fig. 1), which is a

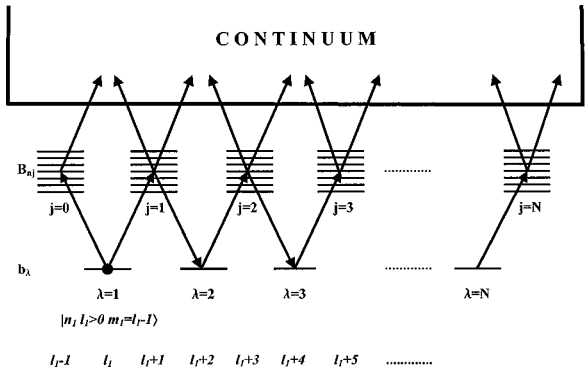

FIG. 1. Model of two-photon ionization of the hydrogen atom by light linearly polarized from the $|\lambda=1\rangle=|n_1,l_1>0,\ m_1=l_1-1\rangle$ state via high-n Rydberg states, extended to include resonant Raman migration of the population from the directly excited Rydberg band ($j=1$) toward higher-l Rydberg bands ($j=2-N$) via states $\lambda=2,3,...,N$ of the same energy as the initial state but different angular momenta.

low excited state of nonzero angular momentum and a specifically chosen projection of the angular momentum. Being in this state, the atom is exposed to a laser beam of linear polarization along the z axis, and a frequency that ensures a band of high-Rydberg states are excited by one-photon absorption. These high Rydberg states are then one photon ionized well above the threshold. Due to the choice of $l_1>0$, the directly excited Rydberg bands are specified by the angular momentum quantum numbers l_1-1 and l_1+1, respectively, but these two bands evolve further along different lines. Because of the assumption of $m_1=l_1-1$, the population from the l_1-1 band is (by the selection rule $\Delta m=0$) forbidden from migrating toward Rydberg bands of angular momentum numbers lower than l_1-1. However, migration from the other l_1+1 band toward a Rydberg band of a higher angular momentum number is allowed, namely, toward that of the number l_1+3, through the resonant state of $n=n_1$ and $l=l_1+2$. If n_1 and l_1, the quantum numbers of the initial state, are chosen properly (relatively high n_1, relatively low l_1), multiple Raman resonances will take place through which the population from the directly excited Rydberg band of the angular momentum number l_1+1 will migrate toward Rydberg bands of much higher angular momenta. For instance, if $n_1=8$ and $l_1=1$ [the case of the $8p(m_1=0)$ initial state is to be considered in detail later on], one encounters as many as three such Raman resonances which give the opportunity for population migration from the Rydberg band of an angular momentum quantum number equal to 2 to higher-l Rydberg bands of $l=4$, 6, and 8. In this case the resonant intermediares are the states sharing the same $n_1=8$, but differing in angular momentum numbers l, which are 3, 5 and 7, respectively.

Let $\lambda=1,2,3,...,N$ number the initial state ($\lambda=1$) and the states orbitally degenerated with it, employed in the process ($\lambda=2-N$). If $l_1>0$ is the angular momentum quantum number of the initial state, the angular momentum of a given λ state is determined by $l_\lambda=l_1+2(\lambda-1)$. We introduce b_λ for the time-dependent Schrödinger population amplitude of the λ state, and $\tilde{b}_\lambda$ for the corresponding Laplace transform. By $j=0,1,2,...,N$, we denote the excited Rydberg bands of the corresponding angular momentum quantum numbers $l_j=l_1+2j-1$. By B_{nj}, we label the time-dependent Schrödinger amplitude for the nth Rydberg state in the jth band, and by $\tilde{B}_{nj}$ we label the appropriate Laplace transform. Finally, we take $\Omega_{\lambda,nj}$ to denote the resonance Rabi frequency for the transition from the λ state to the n state in the j band, and $D_{nj,n'j}$ to denote the Raman coupling via the continuum between any pair of Rydberg states from the same band (all $D_{nj,n'j'}$, with $j'=j\pm1$ are set equal to zero throughout the paper due to their negligibility when compared to the resonant Raman couplings via the λ states [1]). It is well known [2] that, for $n\gg1$, both $\Omega_{\lambda,nj}$ and $D_{nj,n'j}$ scale as the appropriate powers of the principal quantum number of high Rydberg states [$n^{-3/2}$ and $(nn')^{-3/2}$, respectively]. Thus we are allowed to base our solution scheme on the factorization ansatz $\Omega_{\lambda,nj}=f_n\Omega_{\lambda j}$ and $D_{nj,n'j}=f_nf_{n'}D_{jj}$, with f_n being the scaling factor. With this ansatz, we write the coupled algebraic equations for the Laplace transforms of the Schrödinger amplitudes of the discrete states of the model in Fig. 1. In the standard rectangular pulse and rotating-wave approximations, and with the neglect of the continuum-continuum transitions, the equation for $\tilde{b}_\lambda$, obtained along the line presented in Ref. [1], is

$$s\tilde{b}_\lambda=\delta_{\lambda1}-i\Omega_{\lambda\,\lambda-1}K_{\lambda-1}-i\Omega_{\lambda\,\lambda}K_\lambda, \tag{1}$$

where

$$K_j=\sum_n f_n\tilde{B}_{nj}\quad(j=\lambda-1,\lambda), \tag{2}$$

s is the Laplace variable, and $\delta_{\lambda1}$ is the Kronecker symbol reflecting the initial condition for the state populations. Under the same approximations, the appropriate equation for $\tilde{B}_{nj}$ looks like

$$\tilde{B}_{nj}=\frac{-f_n}{s-i\Delta_{nj}}\,(i\Omega_{jj}\tilde{b}_j+i\Omega_{j+1j}\tilde{b}_{j+1}+D_{jj}K_j), \tag{3}$$

with the restriction that $\Omega_{00}=0$ and $\Omega_{N+1N}=0$ due to the nonexistence of the $\lambda=0$ and $\lambda=N+1$ states in our model (see Fig. 1). Moreover, Δ_{nj} is the detuning of the laser frequency from the transition frequency between the initial state and the n state in the j band. It is independent of j in a real hydrogen atom due to the actual degeneracy with regard to the angular momentum quantum number.

In the first step, we multiply Eq. (3) by f_n, and then sum the result over all Rydberg states in a given band, which gives

$$K_j=-iP_jG_j(\Omega_{jj}\tilde{b}_j+\Omega_{j+1\,j}\tilde{b}_{j+1}), \tag{4}$$

where

$$P_j=\sum_n\frac{f_n^2}{s-i\Delta_{nj}} \tag{5}$$

and

$$G_j=\frac{1}{1+P_jD_{jj}}. \tag{6}$$

In terms of K_j and P_j, Eq. (3) reads

$$\tilde{B}_{nj}=\frac{f_n}{s-i\Delta_{nj}}\frac{K_j}{P_j}. \tag{7}$$

In the next step, we substitute K_j of Eq. (4) into Eq. (1), and convert the latter equation into the one for $\tilde{b}_\lambda$ alone. The resulting equation for $\tilde{b}_\lambda$ appears to be of the matrix form

$$\sum_{\lambda'=\lambda,\lambda\pm1} M_{\lambda\lambda'}\tilde{b}_{\lambda'}=\delta_{\lambda 1}, \tag{8}$$

with the matrix elements

$$M_{\lambda\,\lambda-1}=P_{\lambda-1}G_{\lambda-1}\Omega_{\lambda-1\,\lambda-1}\Omega_{\lambda\,\lambda-1}\quad(\lambda\geqslant 2), \tag{9}$$

$$M_{\lambda\,\lambda}=s+P_{\lambda-1}G_{\lambda-1}\Omega^2_{\lambda\,\lambda-1}+P_\lambda G_\lambda\Omega^2_{\lambda\lambda}=A_\lambda, \tag{10}$$

$$M_{\lambda\,\lambda+1}=P_\lambda G_\lambda\Omega_{\lambda\lambda}\Omega_{\lambda+1\,\lambda}=B_\lambda\quad(\lambda\leqslant N-1). \tag{11}$$

This means that the $N\times N$ matrix $M=[M_{\alpha\beta}]$ is of a tridiagonal form, i.e., a form with nonzero elements only on the main diagonal and two neighboring diagonals, one above and the other below the main diagonal. It is easy to see that, by a formal replacement $\lambda\rightarrow\lambda+1$ in Eq. (9), the right-hand side of the transformed equation (9) is made equal to the right-hand side of Eq. (11). Thus the matrix M appears to be not only tridiagonal but also symmetric. In terms of A_λ and B_λ, defined by Eqs. (10) and (11), respectively, this matrix is represented as

$$M=\begin{bmatrix} A_1 & B_1 & 0 & \cdot & \cdot & \cdot & \cdot & & \\ B_1 & A_2 & B_2 & & & & & & \\ 0 & B_2 & A_3 & & & & & & \\ \cdot & & & \cdot & & & & & \\ \cdot & & & & \cdot & & & & \\ \cdot & & & & & \cdot & & & \\ & & & & & & A_{N-1} & B_{N-1} \\ & & & & & & B_{N-1} & A_N \end{bmatrix}. \tag{12}$$

The above matrix significantly differs from the formally similar tridiagonal matrices which appeared many times in the past in the study of different quantum-mechanical and classical problems [3]. The difference is that, instead of being certain constants, our $A_\lambda-s$ and B_λ still depend on the Laplace variable. This will be the origin of serious trouble not encountered in the past. However, irrespective of what $A_\lambda-s$ and B_λ are, the matrix M of Eq. (12) satisfies the known [3] recurrence relation

$$M_\lambda=A_\lambda M_{\lambda-1}-B^2_{\lambda-1}M_{\lambda-2} \tag{13}$$

($M_0=1$, $M_{-1}=0$, $B_0=0$), where M_λ denotes the principal minor of rank $\lambda=1,2,\ldots,N$, i.e., a determinant obtained from the main determinant $M_N=\det M$ by leaving in M_N the first λ rows and columns. This relation is made proved by the application of the Laplace expansion procedure to the last column of M_N. It can be conveniently used to create the main determinant M_N, which is a common denominator in the expressions for $\tilde{b}_\lambda$ solving Eq. (8).

The last step is to find, from $M_N=0$, the poles contributing to the inverse Laplace transformation $\tilde{b}_\lambda\rightarrow b_\lambda$. In general, this is a cumbersome task (numerical, in principle) due to the large dimensionality of the employed basis of states and the actual s dependence of both $A_\lambda-s$ and B_λ. Fortunately, having found the time-dependent originals b_λ, one can apply the Borel convolution theorem [4] when searching the time-dependent amplitudes B_{nj}. This is possible because Eq. (7) for the Laplace transform $\tilde{B}_{nj}$ is recognized as being composed of the products of two different Laplace transforms, one being $\tilde{b}_\lambda$ and the other $\tilde{g}=G_j/(s-i\Delta_{nj})$. If $\tilde{b}_\lambda\rightarrow b_\lambda$ and $\tilde{g}\rightarrow g$, then the inverse Laplace transform of the product $\tilde{b}_\lambda\tilde{g}$ is known to be equal to the convolution $b_\lambda * g$ of the originals b_λ and g, namely,

$$\tilde{b}_\lambda\tilde{g}\rightarrow b_\lambda * g=\int_0^t b_\lambda(t')g(t-t')dt'. \tag{14}$$

We will find this convolution theorem very useful throughout the rest of this paper.

III. ANALYTICAL LIMIT OF THE MODEL

A. Approximation of *l*-independent couplings

We now idealize the model to find some illustrative fully analytical solutions. Analytical solutions to the problems of quantum dynamics in idealized model systems provide qualitative insight into the behavior of real systems. Only with these solutions are we often able to understand the results of the *ab initio* numerical calculations performed for real systems. The idealization we make is that the Rabi frequencies $\Omega_{\lambda j}$ and the Raman couplings D_{jj} are set independent of the angular momentum quantum number l ($\Omega_{\lambda j}=\Omega$ and $D_{jj}=D$). This idealization is known [5] to overestimate the couplings in the case of large-l numbers. With $P_j=P$ in the hydrogen atom (due to the level degeneration), the above assumption leads to a universal j-independent $G=G_j$. As a result, all the diagonal elements in the matrix M of Eq. (12) become equal ($A_1=A_2=\cdots=A_N=A=s+2PG\Omega^2=s+2B$), and the same holds for all the off-diagonal elements ($B_1=B_2=\cdots=B_{N-1}=PG\Omega^2=B$). This allows us to adapt to our aims the solution line invented in Refs. [3] and [5] in the context of different problems. We define

$$\phi=\arccos\left(\frac{A}{2B}\right)=\arccos\left(1+\frac{S}{2B}\right), \tag{15}$$

and, following Ref. [5], we write the solution to Eq. (8) as

$$\tilde{b}_\lambda=\frac{(-1)^{\lambda+1}}{B}\frac{\sin[(N+1-\lambda)\phi]}{\sin[(N+1)\phi]}=\frac{(-1)^{\lambda+1}}{B}F_\lambda. \tag{16}$$

The poles of F_λ are to be determined from

$$\frac{A}{2B}=1+\frac{s}{2B}=\cos\left(\frac{k\pi}{N+1}\right),\quad k=1,2,...,N, \tag{17}$$

and if B was an s-independent constant, these poles would be the only poles of $\tilde{b}_\lambda$, and the problem would become mathematically similar to that in the above-mentioned paper [5].

However, our B depends on s through P, and, for a given k, Eq. (17) becomes an equation with respect to s, which has $p>1$ solutions. We introduce $s_{p,k}$ to denote these solutions. Then the residuum $R^\lambda_{p,k}$ of F_λ at $s_{p,k}$ is found to be

$$\begin{aligned}R^\lambda_{p,k}&=\Omega^2\left(\frac{PG}{1-s\dfrac{G}{P}\dfrac{dP}{ds}}\right)_{s=s_{p,k}}\\&\quad\times(-1)^{k+1}\frac{2}{N+1}\sin\left(\frac{k\pi}{N+1}\right)\sin\left[\frac{N+1-\lambda}{N+1}k\pi\right]\\&=\Omega^2C^\lambda_{p,k},\end{aligned} \tag{18}$$

giving the basis to the fractional decomposition of the function F_λ. On the other hand, $B^{-1}=(D+P^{-1})/\Omega^2$, with

$$P^{-1}=\frac{\Pi_n(s-i\Delta_n)}{\Sigma_{n'}f^2_{n'}\Pi_{n\neq n'}(s-i\Delta_n)}=\frac{f_1(s)}{g(s)}, \tag{19}$$

i.e., a ratio of two polynomials with respect to s, with the polynomial in the numerator being an order higher than the polynomial in the denominator. We divide these polynomials, with the result

$$P^{-1}=\frac{f_1(s)}{g(s)}=\alpha+\beta s+\frac{f_2(s)}{g(s)}, \tag{20}$$

where α and β are some s-independent parameters, and $f_2(s)$ is a polynomial of a lower order than $g(s)$. Then, denoting by s_q the poles of the rational function $f_2(s)/g(s)$, and by R_q the appropriate residua of this function at the above poles, we decompose the function in question in terms of the elementary fractions. All this permits the following representation for $\tilde{b}_\lambda$ of Eq. (16):

$$\tilde{b}_\lambda=(-1)^{\lambda+1}\sum_p\sum_{k=1}^{N}\left(D+\alpha+\beta s_{p,k}+\sum_q\frac{R_q}{s-s_q}\right)\frac{C^\lambda_{p,k}}{s-s_{p,k}}. \tag{21}$$

Finally, applying the convolution theorem [Eq. (14)], one converts the above $\tilde{b}_\lambda$ into the time-dependent amplitude b_λ:

$$b_\lambda=(-1)^{\lambda+1}\sum_p\sum_{k=1}^{N}\left(D+\alpha+\beta s_{p,k}+\sum_q R_q f(s_q-s_{p,k},t)\right)C^\lambda_{p,k}e^{s_{p,k}t}, \tag{22}$$

where $f(x,t)=(e^{xt}-1)/x$.

To find the time-dependent amplitudes B_{nj} we recall Eq. (7), and note that for $j=0$ and $j=N$ (i.e., the first and last Rydberg bands in the model) this equation takes a structurally different form than for all other $j=1,2,...,N-1$, due to $\Omega_{00}=0$ and $\Omega_{N+1N}=0$, respectively. Bearing this in mind and applying the l-independent coupling approximation [Eqs. (15)–(20)], we find, from Eqs. (7) and (4), that, for $j=0$,

$$\tilde{B}_{no}=\frac{-if_n\Omega}{s-i\Delta_n}G\tilde{b}_1=-if_n\Omega\tilde{T}_{n1}; \tag{23}$$

for $j=N$,

$$\tilde{B}_{nN}=\frac{-if_n\Omega}{s-i\Delta_n}G\tilde{b}_N=-if_n\Omega(-1)^{N+1}\tilde{T}_{nN}; \tag{24}$$

and for $j=1,2,...,N-1$,

$$\begin{aligned}\tilde{B}_{nj}&=\frac{-if_n\Omega}{s-i\Delta_n}G(\tilde{b}_j+\tilde{b}_{j+1})\\&=-if_n\Omega(-1)^{j+1}(\tilde{T}_{nj}-\tilde{T}_{n\,j+1}),\end{aligned} \tag{25}$$

where

$$\tilde{T}_{n\lambda}=\frac{F_\lambda/\Omega^2}{(s-i\Delta_n)P}=\frac{1}{s-i\Delta_n}\sum_p\sum_{k=1}^{N}\left(\alpha+\beta s_{p,k}+\sum_q\frac{R_q}{s-s_q}\right)\frac{C^\lambda_{p,k}}{s-s_{p,k}}. \tag{26}$$

As a result, the convolution theorem gives the following time-dependent amplitudes B_{nj}:

$$B_{no}=-if_n\Omega T_{n1}, \tag{27}$$

$$B_{nN}=-if_n\Omega(-1)^{N+1}T_{nN}, \tag{28}$$

$$B_{nj}=-if_n\Omega(-1)^{j+1}(T_{nj}-T_{n\,j+1}),\quad j=1,2,...,N-1, \tag{29}$$

where

$$T_{n\lambda}=e^{i\Delta_n t}\sum_p\sum_{k=1}^{N}\Bigg[(\alpha+\beta s_{p,k})f(s_{p,k}-i\Delta_n,t)+\sum_q\frac{R_q}{s_q-s_{p,k}}[f(s_q-i\Delta_n,t)-f(s_{p,k}-i\Delta_n,t)]\Bigg]C^{\lambda}_{p,k}. \tag{30}$$

Equations (22) and (27)–(30) provide us with a tool to study both the time and intensity effects in the redistribution of the initial population over different discrete states of the model with l-independent couplings. By subtracting the global descrete-state population from 1, we have a way to calculate the ionization probability in our model. Below, we confine the application of Eqs. (22) and (27)–(30) to the cases when Eq. (17) gives simple analytical solutions for $s_{p,k}$.

B. Analytically soluble cases

1. The case of $P=f_n^2/(s-i\Delta_n)$

According to Eq. (5), this choice of P corresponds to leaving only one state in each Rydberg band, the state closest to resonance. By taking the reciprocal of P, from Eq. (20) we identify $\alpha=-i\Delta_n/f_n^2$, $\beta=1/f_n^2$ and $f_2(s)/g(s)=0$ [$f_2(s)/g(s)=0$ results in $R_q=0$]. Then Eq. (17) turns out to lead to a quadratic equation with respect to s having the solutions

$$s_{p,k}=\tfrac{1}{2}[-d_n+(-1)^p x_k],\quad p=1,2,$$

$$x_k=\sqrt{d_n^2-8\Omega_n^2 a_k},\quad a_k=1-\cos\left(\frac{k\pi}{N+1}\right)>0,$$

$$d_n=D_n-i\Delta_n,\quad D_n=Df_n^2,\quad \Omega_n=\Omega f_n. \tag{31}$$

With the above $s_{p,k}$ and P, Eq. (18) for $C^{\lambda}_{p,k}$ is found to be equivalent to

$$C^{\lambda}_{p,k}=(-1)^p\frac{f_n^2}{x_k}C^{\lambda}_k, \tag{32}$$

where

$$C^{\lambda}_k=(-1)^{k+1}\frac{2}{N+1}\sin\left(\frac{k\pi}{N+1}\right)\sin\left(\frac{N+1-\lambda}{N+1}k\pi\right). \tag{33}$$

As a result, the key equations of Sec. III A, i.e., Eqs. (22) and (30) are recast to the following closed-form analytical expressions:

$$b_\lambda=(-1)^{\lambda+1}e^{-d_n t/2}\sum_{k=1}^{N}C^{\lambda}_k\left(\frac{d_n}{x_k}\sinh(x_k t/2)+\cosh(x_k t/2)\right) \tag{34}$$

and

$$T_{n\lambda}=2e^{-d_n t/2}\sum_{k=1}^{N}\frac{C^{\lambda}_k}{x_k}\sinh(x_k t/2). \tag{35}$$

In the simplest case of $N=1$, the last two expressions convert into standard expressions of the model of resonant two-photon ionization from a nondegenerate level via a two fold-degenerate level ($j=0,1$) with the coupling via continuum between the $j=0$ and 1 components ignored.

2. The case of $P=s(f_1^2+f_2^2)/(s-i\Delta_1)(s-i\Delta_2)$

This form of P is specific for a pair of states left in each Rydberg band and a laser frequency fixed in such a way that $\Delta_1 f_2^2+\Delta_2 f_1^2=0$. By taking into account that $\Delta_2=\Delta_1-\Delta$, where Δ is the pair separation, one finds the specific frequency to be the one ensuring the detunings

$$\Delta_1=\frac{\Delta}{1+(f_2/f_1)^2},\quad \Delta_2=-\frac{(f_2/f_1)^2}{1+(f_2/f_1)^2}\Delta. \tag{36}$$

The opposite sign of these detunings means that a virtual state is reached from the initial state of the process lying somewhere inbetween the pair of Rydberg states. In the particular case of equal Rabi frequencies ($f_1=f_2$), this virtual state is localized just in the gravity center of the doublet. It is the advantage of such specifically chosen frequency that, only for this frequency, Eq. (17) again converts into a quadratic equation, now with the solutions

$$s_{p,k}=\tfrac{1}{2}[-d+(-1)^p y_k],\quad p=1,2,$$

$$y_k=\sqrt{d^2-8(\Omega_1^2+\Omega_2^2)a_k+4\Delta_1\Delta_2},$$

$$d=D_1+D_2-i(\Delta_1+\Delta_2), \tag{37}$$

leading to

$$C^{\lambda}_{p,k}=(-1)^p\frac{f_1^2+f_2^2}{y_k}C^{\lambda}_k. \tag{38}$$

Moreover, now $P^{-1}=\alpha+\beta s+(R_1/s)$ with $\alpha=-i(\Delta_1+\Delta_2)/(f_1^2+f_2^2)$, $\beta=1/(f_1^2+f_2^2)$, $R_1=R_q=-\Delta_1\Delta_2/(f_1^2+f_2^2)$, and $s_1=s_q=0$. As a result, we convert Eqs. (22) and (30) into relatively simple analytical forms

$$b_\lambda=(-1)^{\lambda+1}e^{-dt/2}\sum_{k=1}^{N} C_k^\lambda\left(\frac{d}{y_k}\sinh(y_kt/2)+\cosh(y_kt/2)\right.$$
$$\left.-\frac{\Delta_1\Delta_2}{y_k}\,e^{dt/2}[f(s_{2,k'}t)-f(s_{1,k'}t)]\right) \tag{39}$$

and

$$T_{n\lambda}=e^{i\Delta_n t}\sum_{k=1}^{N}\frac{C_k^\lambda}{y_k}\sum_{p=1}^{2}(-1)^p\Big[[s_{p,k}-i(\Delta_1+\Delta_2)]$$
$$\times f(s_{p,k}-i\Delta_{n'}t)-\frac{\Delta_1\Delta_2}{s_{p,k}}[f(s_{p,k}-i\Delta_{n'}t)$$
$$-f(-i\Delta_{n'}t)]\Big], \tag{40}$$

where $n=1,2$.

3. The case of $P=(\pi/\Delta)f_o^2$

The above P is the first term in the expansion of $P=(\pi/\Delta)f_o^2\coth(\pi s/\Delta)=(\pi/\Delta)(1+\mu)/(1-\mu)$ in a power series of $\mu=\exp(-2\pi s/\Delta)$. This coth representation results from Eq. (5) when one approximates the real Rydberg bands by the Bixon-Joertner bands ($\Delta_n=n\Delta$, $n=0,\pm1,\pm2,...,f_n=f_o$) of states which are equidistant and coupled to other states of the model with n-independent strengths. It is known [1] that the inclusion of only the first term in the expansion implies that the Schrödinger population amplitudes to be obtained are valid for the interaction times t not longer than the characteristic Kepler period $\tau=2\pi/\Delta$ ($t/\tau\leqslant1$). The results obtained in the $P=(\pi/\Delta)f_o^2$ approximation [$\alpha=\Delta/(\pi f_o^2)$, $\beta=0$, $R_q=0$, $s_{p,k}=s_k$], thus restricted to $t/\tau\leqslant1$, are

$$b_\lambda=(-1)^{\lambda+1}\sum_{k=1}^{N}C_k^\lambda e^{s_kt} \tag{41}$$

and

$$T_{n\lambda}=\frac{e^{i\Delta_n t}}{1+(\pi D_o/\Delta)}\sum_{k=1}^{N}C_k^\lambda f(s_k-i\Delta_n,t), \tag{42}$$

where

$$s_k=-2\pi\Delta a_k\frac{(\Omega_o/\Delta)^2}{1+(\pi D_o/\Delta)}, \tag{43}$$

and $\Omega_o=\Omega f_o$, $D_o=Df_o^2$. Then, summing squared modulus of the amplitudes B_{nj} [Eqs. (27)–(29)] over all n, one obtains the fraction W_j of the population transferred to the subsequent Bixon-Joertner bands: For $j=0$,

$$W_0=(2\pi)^2\frac{(\Omega_o/\Delta)^2}{|1+(\pi D_o/\Delta)|^2}\sum_{k,l=1}^{N}C_k^1C_l^1 f\left(z_k^*+z_l,\ \frac{t}{\tau}\right); \tag{44}$$

for $j=N$,

$$W_N=(2\pi)^2\frac{(\Omega_o/\Delta)^2}{|1+(\pi D_o/\Delta)|^2}\sum_{k,l=1}^{N}C_k^NC_l^N f\left(z_k^*+z_l,\ \frac{t}{\tau}\right); \tag{45}$$

and for $j=1,2,...,N-1$,

$$W_j=(2\pi)^2\frac{(\Omega_o/\Delta)^2}{|1+(\pi D_o/\Delta)|^2}\sum_{k,l=1}^{N}(C_k^j-C_k^{j+1})$$
$$\times(C_l^j-C_l^{j+1})f\left(z_k^*+z_l,\ \frac{t}{\tau}\right), \tag{46}$$

where $z_k=2\pi s_k/\Delta$, C_k^λ is given by Eq. (33), and $f(z,t')$ was defined after Eq. (22).

IV. RESULTS AND DISCUSSION

To exemplify the analytical solutions obtained, we focus on the model with $N=4$. This model could imitate the process starting from, e.g., the $|\lambda=1\rangle=|n_1l_1m_1\rangle=|8\,1\,0\rangle$ initial state. In this case, the states degenerated with the initial one, engaged in the process, are $|\lambda=2\rangle=|8\,3\,0\rangle$, $|\lambda=3\rangle=|8\,5\,0\rangle$, and $|\lambda=4\rangle=|8\,7\,0\rangle$. On the other hand, the Rydberg bands directly excited from the initial state are those with $l=0$ and 2, while the higher-l bands to which the population partly migrates via the λ states are determined by $l=4$, 6, and 8. According to Fig. 1, $j=0$, 1, 2, 3, and 4 are prescribed to these Rydberg bands, respectively.

We assume the linearly polarized light pulse to have its frequency resonant to the atomic transition from the initial $8p(m_1=0)$ state to the Rydberg state with $n=40$. As the representative Rabi frequency we choose the one corresponding to the transition $8p(m=0)\rightarrow40d(m=0)$ (with accuracy to the factor of 1.94), i.e., $\Omega_n=\Omega f_n=\Omega/(40)^{3/2}=10^7I^{1/2}$, where I is laser intensity expressed in W/cm^2. The bound-bound radial integral required was calculated by us exactly using the recent recipe of Ref. [6] based on the Laplace-transform approach. We checked, however, that the quasiclassical approximation of Ref. [2], exploiting the WKB functions, gives nearly the same result. On the other hand, the representative Raman coupling between different Rydberg states from the same l band is approximated by $D_{nn'}\simeq D_{nn}=D_n=Df_n^2=D/40^3=(1+iq)\gamma/2=20(1+i20)I$. Here γ is (with accuracy to the factor of 1.49) the arithmetic average of the two partial ionization rates from the directly excited $40d$ Rydberg state to p and f continua, at the above assumed frequency, while q is taken in analogy to Ref. [5]. Also in this bound-free case the exact [6] and quasiclassical [2] $d\rightarrow f$ radial integrals were checked to be close to each other. In the case of the Bixon-Joertner structure, we set $\Delta=6.5\times10^{11}$ s^{-1} corresponding to the frequency separation of the $n=40$ level from the nearest neighbor. This leads to the representative Kepler period of the band of excited Rydberg states equal to $\tau=2\pi/\Delta=9.7$ ps. For the above atomic parameters (Ω_n, D_n, and Δ) and three pulse durations, none exceeding the Kepler period ($t/\tau=0.08$, 0.5, and 1), we show in Figs. 2–4 the results obtained from the model with only

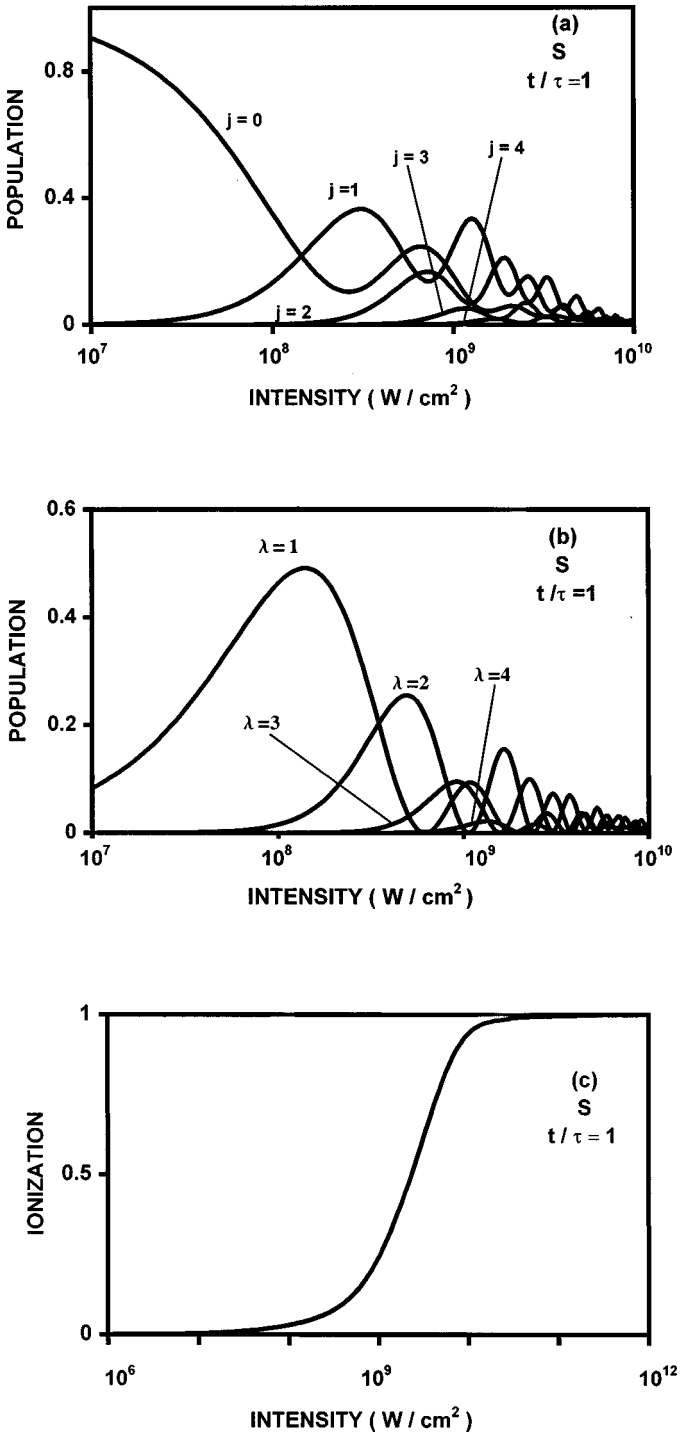

FIG. 2. Population vs laser intensity in the λ-states (a), j Rydberg bands (b), and atomic continuum (c), obtained from the model with $N=4$ and only one state included in each Rydberg band (S), for the pulse duration $t=0.08\tau$, with $\tau=9.7$ ps being the Kepler period of the resonantly excited Rydberg state of $n=40$.

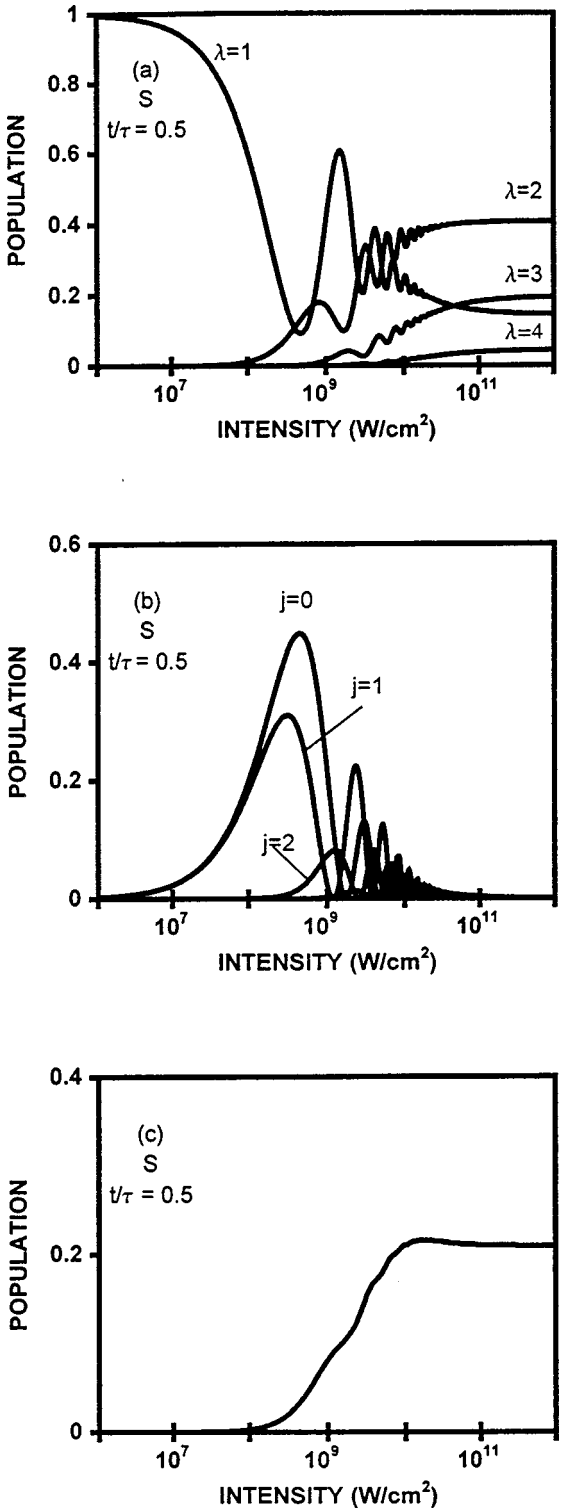

FIG. 3. Same as in Fig. 2, but for $t=0.5\tau$.

one state included in each Rydberg band, while in Figs. 5–7 the corresponding results obtained from the model with the excited Rydberg bands approximated by the Bixon-Joertner structure. In these two opposite limits as to the number of states included in each Rydberg band, the figures in question show the effect of laser intensity on the population of the λ states (a), the Rydberg bands (b), and the atomic continuum (c). We have refrained from presenting the appropriate figures obtained from the model with a pair of states in each Rydberg band, because they resemble to a great extent Figs. 2–4. Figures 2–7 provide a basis to formulate the following main conclusions.

Irrespective of the number of states included in the excited Rydberg bands, the initial state of the process reveals

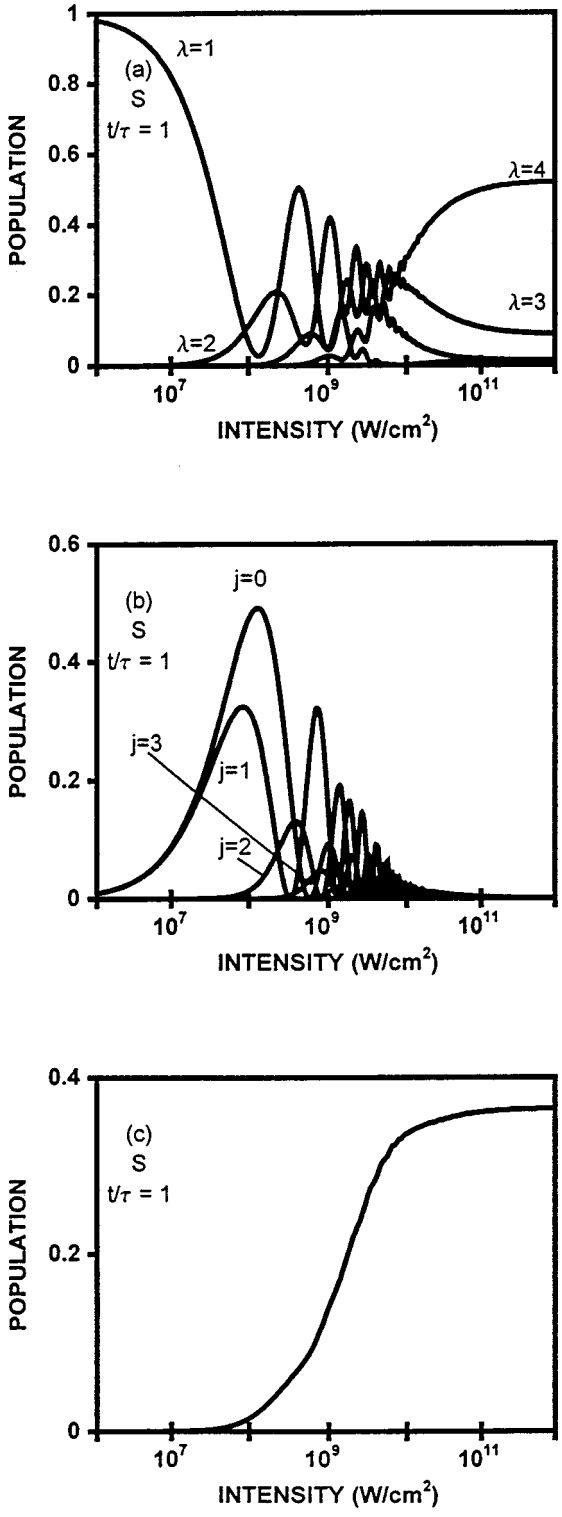

FIG. 4. Same as in Fig. 2, but for $t=1\tau$.

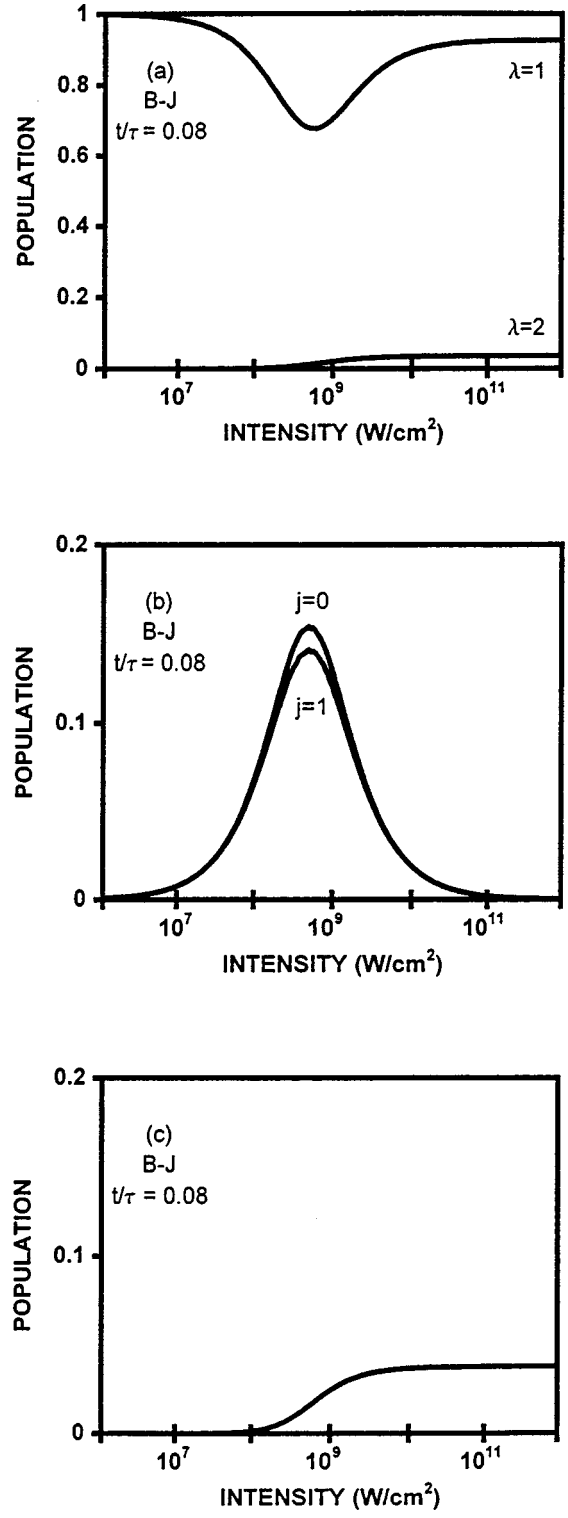

FIG. 5. Population vs laser intensity in the λ states (a), j Rydberg bands (b) and atomic continuum (c), obtained from the model with $N=4$ and each Rydberg band approximated by the Bixon-Joertner structure ($B-J$) for the pulse duration $t=0.08\tau$, with $\tau=9.7$ ps being the Kepler period of the resonantly excited Rydberg state of $n=40$.

the tendency to survive the laser pulse even if it is of high intensity. However, the residual high-intensity population of the initial state becomes smaller and smaller when the pulse duration increases, and drops practically to zero if the pulse duration becomes equal to the Kepler period of the Rydberg state resonantly excited from the initial state.

The initially empty λ states of $\lambda=2-N$, degenerated with the initial state of the process ($\lambda=1$), are populated after the pulse. The population sent to different λ states reaches a relatively high level if the pulse is not too short. Each λ state of $\lambda=2-N$ exhibits the property of trapping the population in an amount which becomes constant after the intensity crosses some threshold value. This seems to be

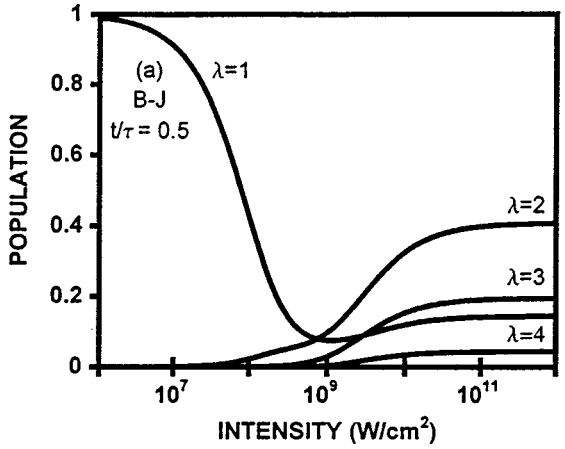

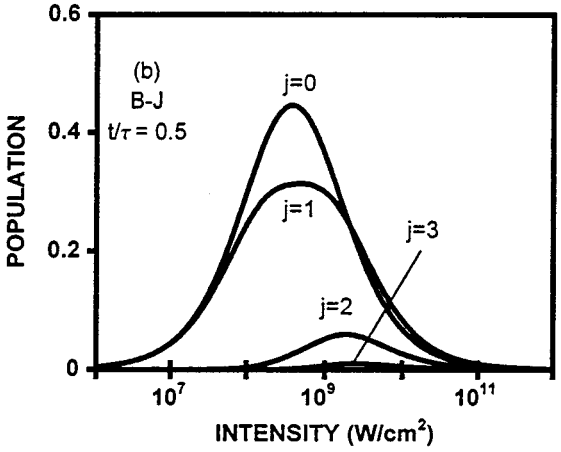

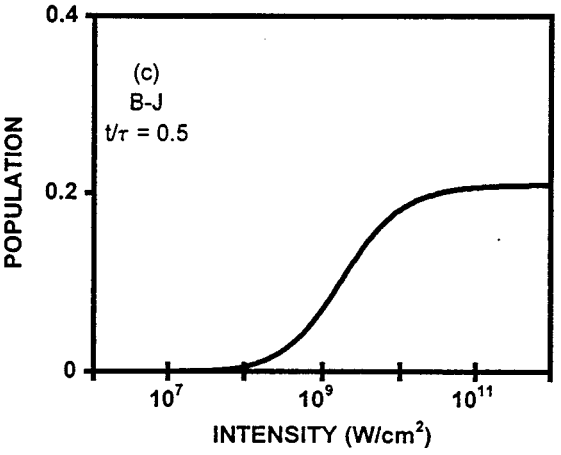

FIG. 6. Same as in Fig. 5, but for $t=0.5\tau$.

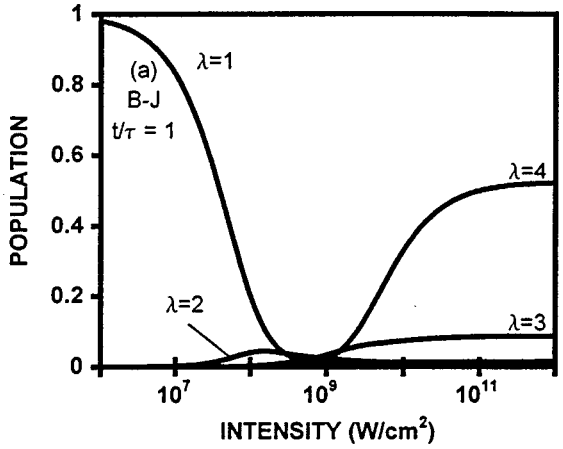

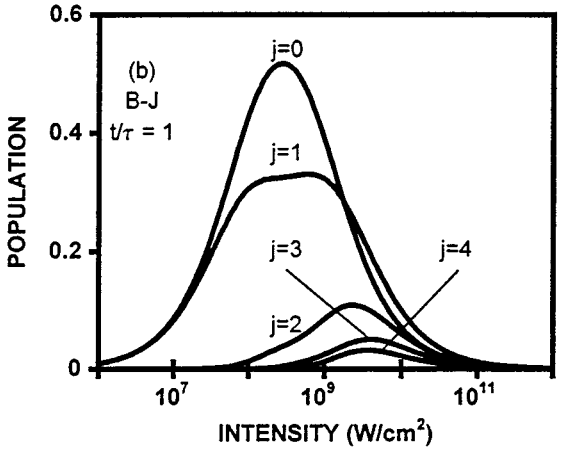

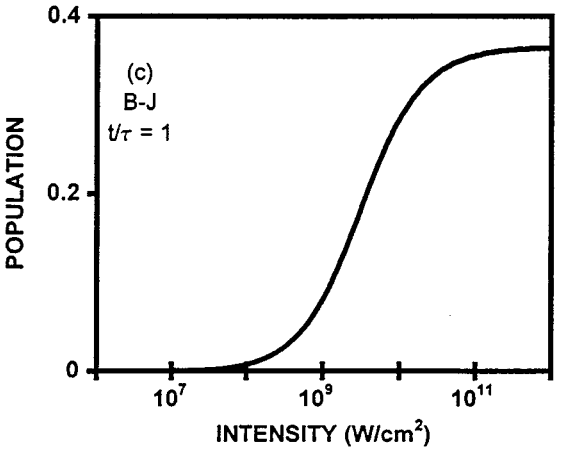

FIG. 7. Same as in Fig. 5, but for $t=1\tau$.

the normal picture when the population trapped in a state with a smaller λ is larger than the population trapped in a state with a higher λ. However, an abnormal picture is possible as well, particularly at longer pulses, when the population is cumulated in high-λ rather than low-λ states (compare the case of $t/\tau=1$ with that of $t/\tau=0.5$).

Qualitatively different from the behavior of the λ states is the behavior of the total population in Rydberg bands, both in bands directly coupled to the initial state and in the higher l bands. The striking difference is that the Rydberg bands are made practically empty at high intensities, i.e., they do not trap population in this intensity limit. A substantial population of the Rydberg bands is reached only at intermediate intensities, particularly at the intensity for which the population of the initial state drops to its main minimum. For these intensities, a non-negligible migration of population from the directly excited Rydberg bands to higher-l Rydberg bands

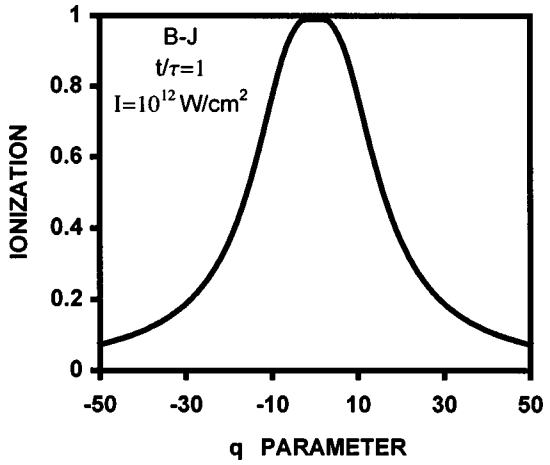

FIG. 8. Ionization by the high-intensity pulse (10^{12} W/cm^2) of the duration $t/\tau=1$ vs parameter q, for the model with a Bixon-Joertner structure of Rydberg bands and $N=4$ (three V-type resonances).

via the λ states of $\lambda \geqslant 2$ takes place if the pulse duration is not too short.

A direct consequence of the above-described behavior of population in discrete states is the observed stabilization of the ionization at a level lower than unity at high intensities. The high-intensity stabilization has its origin in two effects—the effect of survival of the initial state, and the effect of trapping of the population in the states orbitally degenerated with the initial state of the process. The pulse duration determines which of the two effects dominates: for short pulses, it is the effect of survival of the initial state, while for longer pulses, the initial state is made greatly depleted and the trapping of population in the λ states of $\lambda \geqslant 2$ is the prevailing effect.

The above conclusions were derived from the analysis of Figs. 2–7 prepared under a specifically chosen imaginary part in the representative Raman coupling parameter $D_{nn'} = (1+iq_{nn'})\sqrt{\gamma_n \gamma_{n'}}/2 \simeq D_{nn} = (1+iq_n)\gamma_n/2 = 20(1+iq)I$, namely, $q=20$ in analogy to Ref. [5]. We have varied the parameter q over a wide range, and found that its change substantially affected the shape of some curves from Figs. 2–7. The curves most resistant to the change of q turned out to be those of the total population of Rydberg bands [parts (b) in Figs. 2–7]. However, the population in both λ states [parts (a) in Figs. 2–7] and atomic continuum [parts (c) in Figs. 2–7] exhibited remarkable sensitivity to the change of q. The general tendency we observed was that, with diminishing q, less and less population survived in the initial state ($\lambda=1$) and less and less population was trapped in other λ states when the pulse intensity increased. In the limit of $q \rightarrow 0$ no population was left in any of the λ states at high intensities. A direct consequence was a complete ionization in the limit of high intensities (10^{12} W/cm^2), i.e., no evidence of the effect of stabilization when $q \rightarrow 0$. To emphasize this result, in Fig. 8 we present the ionization probability by a pulse of high intensity (10^{12} W/cm^2) and the duration $t/\tau = 1$ in its dependence on parameter q, for the model with $N=4$ and the Bixon-Joertner approximation of Rydberg bands. A curve similar to that of Fig. 8 is obtained when only one state in each Rydberg band is left. Figure 8 points to the necessity of having a large q parameter for obtaining a stabilization in our model of ionization via high Rydberg states. This result of the above model of ionization via high Rydberg states agrees qualitatively with the result of two models (numerical [7] and analytical [8]) of the so-called interference stabilization, i.e., when ionization starts from a high Rydberg state that is directly one photon coupled to the continuum. As a matter of fact, it was shown in Refs. [7, 8] that a nonzero q parameter enhances the interference stabilization.

Of direct relevance to our model of ionization via the high Rydberg state is the recent model of Fedorov and Poluektov [9] of interference stabilization. In this model, a resonance was allowed between the initially populated high Rydberg state and a much lower-lying state, but no migration of population to higher-angular-momentum discrete states was included. This model was considered from the point of view of the competition between Λ-type (i.e., via the continuum) and V-type (i.e., via the lower resonant state) redistributions of the population over large number of high Rydberg states neighboring the initially populated one. An interesting conclusion derived by Fedorov and Poluektov was that, applying pulses much longer than the classical Kepler period of the initial high Rydberg state, one can expect stabilization in weaker fields determined by the condition $\Omega_n = \Delta$ instead in stronger fields determined by either $\mathrm{Re}(D_n)=\Delta$ or $\mathrm{Re}(D_n) = \Omega_n$ (in our case, the critical intensities resulting from these conditions are 4.2×10^9, 3.3×10^{10}, and 2.5×10^{11} W/cm^2, respectively). The origin of the above shift of the threshold of stabilization toward lower intensities lies in the pronounced V-type redistribution, in accordance with, e.g., Fig. 8 in Ref. [10]. A question arising in this context is if an analogous effect of lowering the stabilization threshold emerges from our model of ionization via high Rydberg states when pulses much longer than the Kepler period are considered. In the case of the Bixon-Joertner approximation of Rydberg bands, the answer to this question can be found by taking into account a few terms (instead of the first one only) in the expansion of $P^{-1} = (\Delta/\pi)(1-\mu)/(1+\mu)$ in a power series of $\mu = \exp(-2\pi s/\Delta)$ [10]. With this expansion, Eq. (17) will be converted to include the Laplace variable in the argument of the exponential function as well. Unavoidably, numerical procedures will have to be applied to find the poles $s_{p,k}$. Having these poles, we will be able to find the time-dependent amplitudes b_λ from Eq. (16) by applying the translation theorem [if $f(s) \rightarrow f(t)$, then $e^{-as} f(s) \rightarrow f(t-a)\Theta(t-a)$, where $\Theta(x)$ is the step Heaviside function]. In a similar way we can find the time-dependent amplitudes B_{nj} applying both the translation and convolution theorems to the first part of Eq. (26). As seen, a different solution procedure from that developed in the present paper is needed to consider pulses longer than the Kepler period in the framework of the model in which high Rydberg bands are approximated by the Bixon-Joertner structure. If, however, a large but finite number of states in each Rydberg band is considered, the procedure developed is applicable for longer pulses as well, but, again, numerical solutions to Eq. (17) and equation $g(s)=0$, with $g(s)$ as defined by Eq. (20), are unavoidable. Numerical investigation along the above lines, covering pulses longer than the characteristic Kepler period of the excited Rydberg bands, will be undertaken, and the

results will be presented elsewhere. We hope that these numerical results will answer the question raised at the end of the present paper, whose spirit was analytical in principle.

V. SUMMARY

We presented a generalized model of nominal two-photon ionization of the hydrogenlike atom via a band of high Rydberg states. The generalization consisted of the inclusion of the resonant migration of the population from the directly excited Rydberg band toward higher-angular-momentum Rydberg bands through V-type degenerate Raman transitions, engaging, as resonant intermediares, states of the principal quantum number the same as that of the initial state but of different angular momentum quantum numbers. In the model considered, many V-type resonances were allowed which were linked in a chain of a length dependent on the quantum numbers of the initial state. This chain was the element which differentiated the generalized model presented from the one described earlier in Ref. [1], and from other approaches to ionization via high Rydberg states [11–15]. The generalized model was considered in detail in the idealized limiting case, permitting a completely analytical solution to be found even for an arbitrary length of the chain of the V-type couplings. Though found for the idealized case, our solution seems to be nontrivial, since closed-form analytical solutions are known to be not often obtained when studying the dynamics of transitions in multistate systems exposed to an intense electromagnetic field.

As an illustration, our analytical solution was applied to a system with three V-type resonances. For this system, we studied the effects of intensity and pulse duration on the survival of the initial state of the process, on the migration of population to bound states of higher angular momenta, and on stabilization against ionization. Probably the most important conclusion was that in the limit of high intensities no population was left in high Rydberg states, and, thus, the stabilization was the result of both the initial-state survival and trapping of some population in higher-angular-momentum states of the same energy as the initial state. In this high-intensity limit, the duration of the light pulse was shown to be decisive as to where the population was predominantly left in the atom—either in the initial state, when the pulse was short, or in the states orbitally degenerated with the initial state, when the pulse was longer. It was shown, however, that the effect of stabilization in our model was highly sensitive to the value of the imaginary part in the parameter $D_{nn'}$ of nonresonant Raman coupling between different high Rydberg states from the same l band.

ACKNOWLEDGMENTS

We gratefully acknowledge support from the Polish Committee for Scientific Research (Grant No. 2 PO3B 078 12) that made this research possible.

[1] A. Wójcik, R. Parzyński, and A. Grudka, Phys. Rev. A **55**, 2144 (1997).
[2] M. S. Adams, M. V. Fedorov, V. P. Krainov, and D. D. Meyerhofer, Phys. Rev. A **52**, 125 (1995).
[3] Z. Białynicka-Birula, I. Białynicki-Birula, J. H. Eberly, and B. W. Shore, Phys. Rev. A **16**, 2048 (1977), and references therein.
[4] D. G. Zill, *Differential Equations with Boundary—Value Problems* (PWS, Boston, 1986), p. 310.
[5] R. Grobe, G. Leuchs, and K. Rzążewski, Phys. Rev. A **34**, 1188 (1986).
[6] G. Feldman, T. Fulton, and B. R. Judd, Phys. Rev. A **51**, 2762 (1995).
[7] M. V Fedorov, M. M. Tehranchi, and S. M. Fedorov, J. Phys. B **29**, 2907 (1996).
[8] R. Parzyński and A. Wójcik, Laser Phys. **7**, 551 (1997).
[9] M. V. Fedorov and N. P. Poluektov, Laser Phys. **7**, 299 (1997); Opt. Express **2**, 51 (1998) (http://epubs.osa.org/opticsexpress).
[10] A. Wójcik and R. Parzyński, Phys. Rev. A **50**, 2475 (1994).
[11] B. Piraux, E. Huens, and P. L. Knight, Phys. Rev. A **44**, 721 (1991).
[12] E. Huens and B. Piraux, Phys. Rev. A **47**, 1568 (1993).
[13] F. H. M. Faisal and L. Dimou, Acta Phys. Pol. A **86**, 201 (1994).
[14] M. Yu Ivanov, Phys. Rev. A **49**, 1165 (1994).
[15] J. D. Corless and C. R. Stroud, Jr., Phys. Rev. Lett. **79**, 637 (1997).